حسگر ضریب شکست بر مبنای دو صفحه گرافین و تشدیدگر استوانه‌ای گرافینی

سمیه عسگری[۱] و نصرت ا... گرانپایه[۱]

۱-دانشکده مهندسی برق، دانشگاه صنعتی خواجه نصیرالدین طوسی، تهران، ایران

چکیده – در این مقاله، عملکرد یک حسگر ضریب شکست گرافینی با یک تشدیدگر استوانه‌ای را با استفاده از روش تفاضل محدود در حوزه‌ی زمان بررسی و شبیه‌سازی کرده، و حساسیت حسگر را برای بررسی عملکرد آن محاسبه کرده‌ایم. از این ساختار می‌توان برای طراحی و ساخت حسگرهای ضریب شکست در مقیاس نانو استفاده کرد.

کلید واژه- افزاره‌های پلاسمونی، حسگر ضریب شکست، افزاره‌های گرافینی.

A Refractive Index Sensor Based on two Graphene Sheets and Graphene Cylindrical Resonator

Somayyeh Asgari, Nosrat Granpayeh

Faculty of Electrical Engineering, K. N. Toosi University of Technology, Tehran, Iran

Abstract- In this paper, we have proposed and simulated a graphene-based refractive index sensor with a cylindrical resonator, by using the finite-difference time-domain method. The sensor sensitivity has been derived to show its sensing performance. The proposed device can be utilized in design and construction of optical nano-scale refractive index sensors.

Keywords: Graphene devices, Plasmonic devices, Refractive Index Sensor.

This article is valid, only if it has been indexed in www.opsi.ir.

A Refractive Index Sensor Based on two Graphene Sheets and Graphene Cylindrical Resonator

Somayyeh Asgari

s_asgari@ee.kntu.ac.ir

Nosrat Granpayeh

granpayeh@kntu.ac.ir

1   Introduction

Graphene, a two dimensional material with a honey comb lattice, has become attractive because of its remarkable optical features such as low loss, small size, and tunable conductivity [1, 2]. Graphene, a plasmonic material, has been utilized for constructing nano-scale optical devices and systems [3].

Recently, different types of graphene plasmonic devices, such as filters [4], sensors [5], and splitters [6] have been proposed and analyzed. A single graphene layer supports two kinds of surface plasmon polariton (SPP) modes: waveguide modes, in which the field is confined along the entire area of the layer, and edge modes, in which the field is confined on the rims of the layer [7].

In this paper, by using finite-difference time-domain (FDTD) method, we have designed, analyzed, and simulated an optical graphene-based refractive index sensor. Our structure is composed of two parallel graphene sheets as input and output ports and a graphene cylindrical resonator between them. Our study will improve the construction of nano-scale plasmonic refractive index sensors in the mid-infrared region.

The paper is organized as follows: In Section 2, the structure is proposed and investigated, its refractive index sensitivity is calculated, and simulation results are obtained, and the paper is concluded in Section 3.

2   Structure and Analysis Method

2.1   Description

The schematic view of our proposed sensor is shown in Figure 1. The structure should be inserted in a dielectric medium. We assume that the background of the structure is air in our FDTD simulations. In our simulations, graphene is an ultra-thin layer with a thickness of Δ, which is assumed to be 1 nm in mid-infrared region. The graphene surface conductivity (σ_g) is calculated by the Kubo's formula and it depends on the momentum relaxation time, τ, temperature, T, chemical potential (Fermi energy), μ_c, and incident angular frequency, ω [3]:

$$\sigma_g = i \frac{e^2 k_B T}{\pi\hbar^2(\omega+i\tau^{-1})}\left\{\frac{\mu_c}{k_B T}+2\ln\left[\exp\left(\frac{-\mu_c}{k_B T}\right)+1\right]\right\}$$
$$+ i\frac{e^2}{4\pi\hbar^2}\ln\left[\frac{2|\mu_c|-\hbar(\omega+i\tau^{-1})}{2|\mu_c|+\hbar(\omega+i\tau^{-1})}\right]$$

(1)

where $-e$, k_B, and $\hbar$ are respectively the electron charge, the Boltzmann's constant, and the reduced Planck's constant.

At room temperature, the intraband transition dominates. So, the Kubo's formula simplifies to [3]:

$$\sigma_g = \frac{ie^2\mu_c}{\pi\hbar^2(\omega+i\tau^{-1})}$$

(2)

and the carrier relaxation time is

$$\tau = -\frac{\mu\mu_c}{ev_f^2}$$

(3)

where μ is the carrier mobility and v_f is the Fermi velocity in graphene. The material parameters are assumed as: μ=10,000 cm²/(V.s), $v_f = 10^6$ m/s, and μ_c=0.3 eV. In our simulations, the graphene is assumed as an anisotropic dielectric with the in-plane graphene permittivity as:

$$\varepsilon_{eq} = 2.5 + i\frac{\sigma_g}{\omega\varepsilon_0\Delta}$$

(4)

Where ε_0 is the free space permittivity, and the surface-normal component as ε=2.5, based on the dielectric constant of graphite [9].

2.2   Analytic Method

The inner and the outer radius of the graphene cylindrical resonator are r_1 and r_2, respectively. We assume the average radius of the cylinder as $R = \dfrac{r_1 + r_2}{2}$

The relationship between wavelengths of transmittance peaks and the average radius of resonator can be calculated theoretically by the resonance equation of the cylindrical resonator [9]:

$$\mathrm{Re}(k).2\pi R = 2m\pi$$

(5)

where m is an integer, $k=k_0 n_{eff}$, is the wavenumber of SPPs, n_{eff} is the effective refractive index of the graphene cylinder [9]:

$$n_{eff} = \sqrt{1 - \left(\frac{2}{\eta_0 \sigma_g}\right)^2}$$

(6)

Where η_0 (~377Ω) is the impedance of air and σ_g is the graphene surface conductivity.

2.3 General Aspects of Simulation

Our structure has been simulated by using a two dimensional finite-difference time-domain (2D-FDTD) method, with a 12 perfectly matched layer (PML) absorbing boundary condition. One dipole point source with transverse electric (TE) polarization is placed 2 nm above the input graphene waveguide port to excite the SPP waves propagating along the x direction. Two monitors are placed at the points P_1 and P_2 for measuring the input power, P_{in} and the transmitted power, P_{out}. The transmittance is defined as $T= P_{out} / P_{in}$. We have used a non uniform mesh in our simulations to save computational time of our calculations. The minimum mesh size inside graphene has been assumed 0.1 nm and increases gradually outside the graphene.
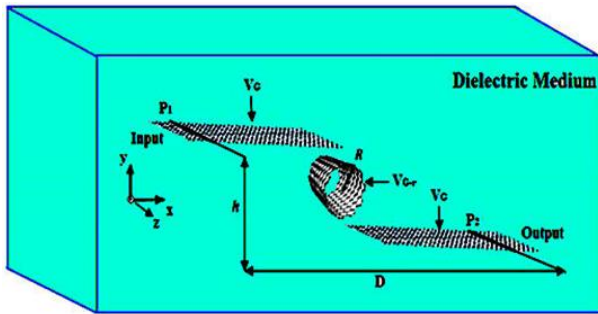

Figure 1: Schematic view of the proposed sensor consists of two graphene sheets as input and output ports, and a graphene cylindrical resonator between them. R is the average radius of the resonator, h is the

distance between two graphene sheets, and D is the distance between two power monitors, P_1 and P_2.

3. Results and Discussion

3.1 Refractive Index Sensor

The cylindrical resonator is filled with dielectric materials with various refractive indices, n, for derivation of refractive index sensitivity. The transmittance spectra with n=1, 1.05, 1.1, 1.15, and 1.2 for R= 99.5 nm, and h=300 nm are plotted in Figure 2(a).

Transmittance peaks show a red shift as n increases. The refractive index sensitivity of the resonance peaks have been calculated by $S=\Delta\lambda/\Delta n$. Our proposed structure shows a high value of 6100 nm per refractive index unit (nm/RIU) sensitivity which is higher than the metal one [9]. In Figure 2(b), the resonance wavelengths of the sensor as a function of the resonator material refractive index for different average radii of the resonator are shown. A comparison shows that the transmittance peaks tend to exhibit a red shift as the resonator radius increases.
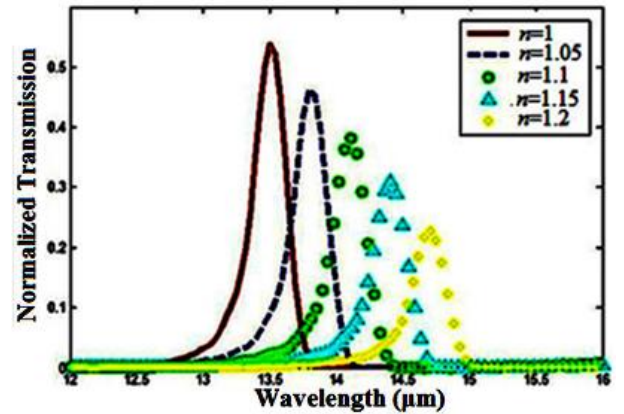
(a)
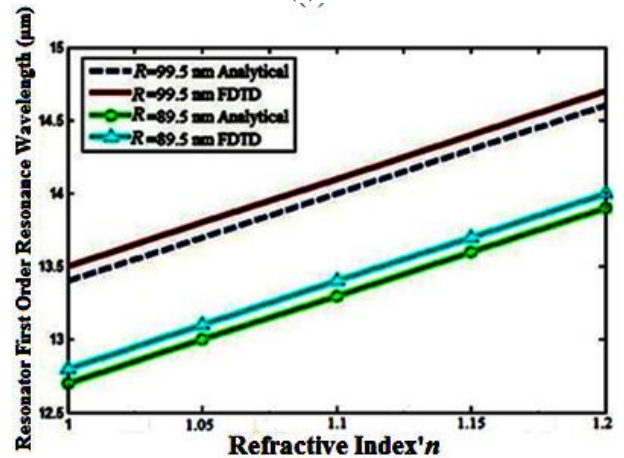
(b)

Figure 2: (a) Normalized transmission spectra of the refractive index sensor of Figure 1 for five different

values of *n* with *R*=99.5 nm and *h*=300 nm. (b) The first order resonance wavelengths of the resonator versus the resonator material refractive index for various resonator radii.

4. Conclusion

In this paper, two parallel graphene sheets separated by a graphene cylindrical resonator are proposed analytically and numerically for the refractive index sensor. The sensor is analyzed by the two dimensional finite-difference time-domain (2-D FDTD) method. The shifts of the transmission peaks have a linear relation with the refractive index of the material inside the resonator. The device is simple and has high refractive index sensitivity compared to the metal one and also it has smaller size than the metal one. It also has extensive potential applications in bio-sensing. Our structure can be used in design of nano-plasmonic refractive index sensors.

References

[1] Q. Bao and K. P. Loh, "Graphene photonics, plasmonics, and broadband optoelectronic devices," *ACS. Nano*. Vol. 6, No. 5, pp. 3677-3694, 2012.

[2] S. Tavasolmand and M. Hashemi, "Tunable graphene absorber by applying external gate voltage," *The 22nd ICOP, and the 9th ICPET*. pp. 384-387, 2016.

[3] P. Li and T. Taubner, "Broadband subwavelength imaging using a tunable graphene-lens," *ACS. Nano*. Vol. 6, No. 11, pp. 10107-10114, 2012.

[4] M. Danaeifar, N. Granpayeh, A. Mohammadi, and A. Setayesh, "Graphene-based tunable terahertz and infrared band-pass filter," *Appl. Opt*. Vol. 52, No. 22, pp. 68-72, 2013.

[5] S-B. Yan, L. Luo, C-Y. Xue, and Zhi-Dong Zhang, "A Refractive Index Sensor Based on a Metal-Insulator-Metal Waveguide-Coupled Ring Resonator," *Sensors*. Vol. 15, No. 11, pp. 29183-29191, 2015.

[6] X. Zhu, W. Yan, N. A. Mortensen, and S. Xiao, "Bends and splitters in graphene nanoribbon waveguides," *Opt. Express*. Vol. 21, No. 3, pp. 3486 (1-6), 2013.

[7] J-P. Liu, X. Zhai, L-L. Wang, H-J. Li, F. Xie, Q. Lin, and S-X. Xia, "Analysis of mid-infrared surface plasmon modes in a graphene-based cylindrical hybrid waveguide," *Plasmonics,* Vol. 11, No. 3, pp. 703-711, 2016.

[8] W. Gao, J. Shu, C. Qiu, and Q. F. Xu, "Excitation of plasmonic waves in graphene by guided-mode resonances," *ACS Nano*. Vol. 6, No. 9, pp. 7806–7813, 2012.

[9] X. Xia, J. Wang, F. Zhang, Z. Hu, C. Liu, X. Yan, and L. Yuan "A nanoscale refractive index sensor based on asymmetric plasmonic waveguide with a ring resonator," *IEEE. Sens. J.* Vol. 17, No. 26, pp. 24096-24101, 2014.

This article is valid, only if it has been indexed in www.opsi.ir.